Inorganic Chemistry

Article

pubs.acs.org/IC

Synthesis, Structure, and Catalytic Applications for *ortho*- and *meta*-Carboranyl Based NBN Pincer-Pd Complexes

Min Ying Tsang,[†] Clara Viñas,[†] Francesc Teixidor,[†] José Giner Planas,*[,†] Nerea Conde,[⊥] Raul SanMartin,[⊥] María Teresa Herrero,[⊥] Esther Domínguez,[⊥] Agustí Lledós,[‡] Pietro Vidossich,[‡] and Duane Choquesillo-Lazarte[§]

[†]Institut de Ciència de Materials de Barcelona (ICMAB-CSIC), Campus UAB, 08193 Bellaterra, Spain

[⊥]Department of Organic Chemistry II, University of the Basque Country, 48980 Leioa, Spain

[‡]Departament de Química, Universitat Autónoma de Barcelona, 08193 Bellaterra, Spain

[§]Laboratorio de Estudios Cristalográficos, IACT, CSIC-University of Granada, Armilla, Granada, Spain

Supporting Information

ABSTRACT: *o*- and *m*-Carborane-based NBN pincer palladium complexes (***o*CB-L1)Pd**, (***o*CB-L2)Pd**, and (***m*CB-L1)Pd** are synthesized in two steps from commercially available starting materials. The pincer complexes were prepared by the reaction of bis-[R(hydroxy)-methyl]-1,2-dicarba-*closo*-dodecaborane (R = 2-pyridyl ***o*CB-L1**, 6-methyl-2-pyridyl ***o*CB-L2**) or bis-[2-pyridyl (hydroxy)methyl]-1,2-dicarba-*meta*-dodecaborane (***m*CB-L1**) with $[PdCl_2(MeCN)_2]$ under mild conditions. The X-ray structure determination of all carboranyl pincer complexes shows unambiguously B−H activation of the carborane cages. The results agree with the Pd−B bonds in all complexes exhibiting strong σ-electron donation. Theoretical calculations reveal the importance of considering the solid state intermolecular hydrogen bonding when investigating the *trans* influence in organometallic chemistry. A localized orbitals approach has also been applied to analyze the metal oxidation state in the carboranyl pincer complexes. Catalytic applications of (***o*CB-L1)Pd** and (***m*CB-L1)Pd** have shown the complexes are good catalyst precursors in Suzuki coupling in water and with very low amounts of catalyst loadings.

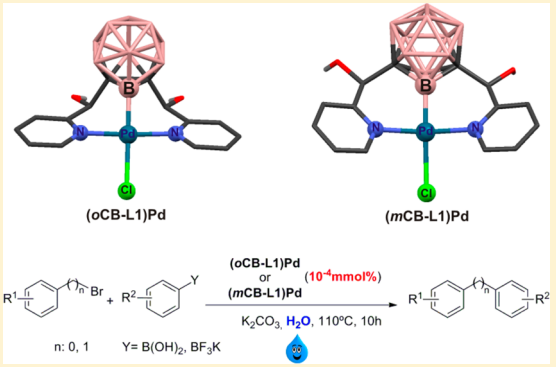

INTRODUCTION

Pincer complexes represent an exciting platform for fundamental studies on transition metal coordination chemistry, metal mediated reactivity, and homogeneous catalysis.[1] Pincer ligands feature a rigid and tridentate binding pocket, usually a coordinating bridgehead position and two donor arms. Side arm functionalization and selection of the coordinating bridgehead position allow careful tuning of desired ligand physical and electronic properties, and finally the pincer complex by selection of the appropriate transition metal.[1] Perhaps the most attractive feature of metal pincer complexes is the unique possibility for fine-tuning the catalytic activity of the metal atom. Since the coordinating bridgehead position is usually coplanar with the coordination site available for catalysis, steric and electronic properties of the pincer ligand can be efficiently transferred to the metal center.[1] The coordinating bridgehead positions are, more often than not, carbon-based,[1,2] but also amido,[3] silyl,[4] or phophido[5] units to provide heterodonor functionality. Boron was surprisingly absent in this picture until work reported by Teixidor[6] in 1991 and later by Nozaki[7] and Mirkin[8] in 2009. Teixidor and co-workers reported the first dithio-7,8-*nido*-carboranyl based SBS pincer rhodium complex, although it was not recognized as such at that time. Nozaki reported the first boryl-based PBP ligand system and showed that the iridium complex of this ligand showed a stronger σ-donating ability, and therefore a stronger *trans* influence, than the corresponding PCP ligand.[7] Concomitant with Nozaki's report, Mirkin and co-workers initiated a new chapter in carborane chemistry by providing the first two *closo*-*meta*-carborane-based (EBE) pincer complexes **1** (E = S) and **2** (E = Se) structures with previously unobserved Pd−B boryl σ-coordination within a pincer ligand framework (Figure 1, top). The latter implies a strong electron-donating ability of the boron moiety and therefore a strong *trans* influence (Pd−Cl distance 2.44 Å).[8]

The development of pincer complexes incorporating boron as a pivotal, ligating element is important for several reasons. In contrast to the class of metallaboratranes, which feature a M(donor)−B(acceptor) bond, these ligands feature a stable, strongly σ-donating boryl fragment.[9] The incorporation of the rich carborane chemistry to the pincer type complexes has now

Received: June 13, 2014
Published: August 11, 2014

   dx.doi.org/10.1021/ic5013999 | *Inorg. Chem.* 2014, 53, 9284−9295

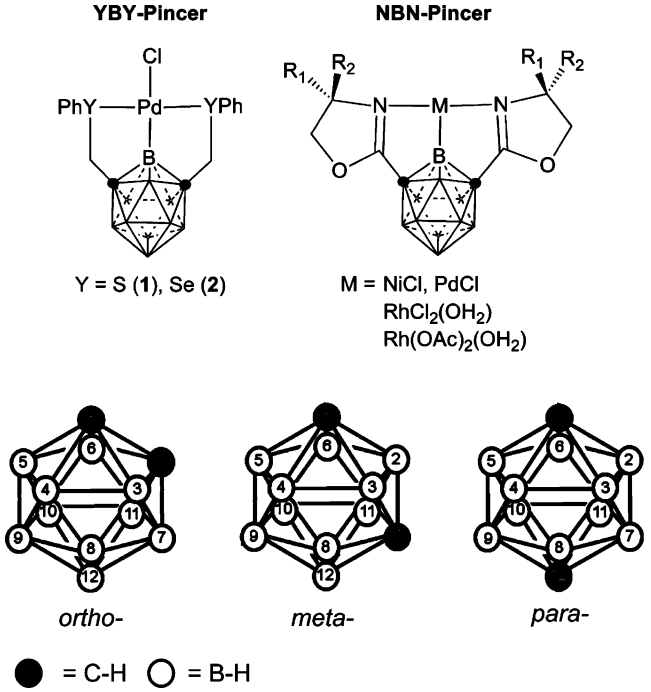

Figure 1. Reported *closo*-carboranyl-based pincers (top) and graphical representation of the caborane isomers (*closo*-$C_2B_{10}H_{12}$) with vertex numbering.

been expanded to include possible applications as ligands in transition metal catalysis. Following Mirkin's report, Nakamura and co-workers reported the synthesis and application in asymmetric catalysis of a new family of *meta*-carborane-based (NBN) pincer complexes (Figure 1, right).[10] All *closo*-carborane-pincer complexes reported so far are based in the *meta*-carborane isomer (Figure 1, bottom), that is, one of the three possible isomers of carborane (*ortho*-, *meta*-, and *para*-*closo*-$C_2B_{10}H_{10}$, from now on *o*-, *m*- and *p*-carborane; Figure 1). Electron density of the vertexes is strongly affected by the different electronegativities between carbon and boron atoms and by their arrangement in the three isomers. Both calculations and chemical reactivity reveal that B(3) (or 6) in *o*-carborane is more positive than the related B(2) (or 3) in *m*-carborane and B atoms in *p*-carborane are practically neutral.[11,12] In other words, the boron atoms attached to both carbon atoms of the cluster are more electron-withdrawing in the *o*-carborane than in the *m*-carborane isomers. The effect is known to transmit to the substitutents at boron, and therefore it should also affect the metal centers in carboranyl based EBE complexes. Providing that this effect is significant, it could provide an exclusive control of electronic properties (such as *trans* influence) over the steric ones by simply selecting the desired carborane isomer for a given carboranyl based ligand and its corresponding EBE complex. Such control in electronic tuning without altering the steric factors is an exclusive feature of carborane based ligands.[13]

During the last few years, we have synthesized and studied the supramolecular structures of a family of mono- and disubstituted chiral *o*-carboranylalcohols (Scheme 1), which are isolated as racemic mixtures.[14] These molecules, which are prepared in very good yields from one-pot reactions and from readily available starting materials, are centered around an *o*-carborane core with one or two arms radiating out of one of the cluster carbons, containing a chiral carbon that bears an alcohol

Scheme 1. Previously Synthesized Carboranylalcohols

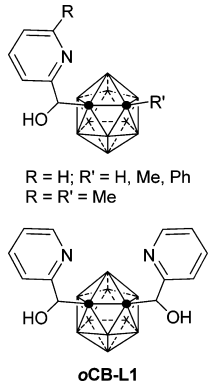

and an aromatic moiety. The high thermal and chemical stability, hydrophobicity, acceptor character, ease of functionalization, and three-dimensional nature of the icosahedral carborane clusters make these new molecules valuable ligands in coordination chemistry.[9a,11b] Thus, soon after we obtained our first *o*-carboranylalcohols we initiated a systematic study of the coordination chemistry of all these monosubstituted *o*-carboranylalcohol ligands, and more recently on our disubstituted ligands, with several transition metals.[15] We obtained a first family of *o*-carboranyl NBN based pincer palladium complexes and extended the synthesis to the corresponding *m*-carboranyl NBN analogues. Here, we report on the structural and electronic characterization of these ligands and the corresponding Pd complexes, and on catalytic properties of the latter.

RESULTS AND DISCUSSION

Synthesis and Characterization of Ligands. Following our previous report,[14d] we have now expanded our family of bis-pyridylmethyl alcohols derived from the *o*-carborane cluster (***o*CB-L2**; Scheme 2) and synthesized a new related *m*-carborane analogue (***m*CB-L1**; Scheme 2). The reaction of dilithiated *o*-carborane or *m*-carborane with the corresponding aromatic aldehydes at low temperature afforded the new ligands in reasonable yields (57−79%). All new compounds have been fully characterized by standard spectroscopic and analytical techniques, and the data correlated well with that of related alcohols.[14] All these compounds contain two chiral centers that can adopt either *R* or *S* configuration and therefore could lead to the formation of two diastereoiseomers, a *meso* compound (*RS*; OH groups in a *syn* orientation) and a racemic compound (mixture of *SS* and *RR*; OH groups in an *anti* orientation). Extensive NMR analysis for *o*-carborane ***o*CB-L1** was done in the previous report and showed that *anti*- and *syn*-diastereoisomers for ***o*CB-L1** showed separated NMR signals. In contrast, the mixture of *anti*- and *syn*-diastereoisomers of ***m*CB-L1** showed a sole set of signals in the ^{1}H NMR spectrum. The latter might be related to free rotation of the pyridylalcohol arms in the *meta*-carborane derivatives, so that an average NMR pattern is observed for the ***anti*-** and ***syn*-*m*CB-L1** mixture. Free rotation of pyridylalcohol arms in *ortho*-carborane derivatives is clearly not possible due to steric hindrance.[14d]

Synthesis of Carborane-Based NBN Pincer Complexes. New pincer complexes (***o*CB-L1)Pd** and (***m*CB-L1)Pd** were synthesized in high yield (71−76%) by reacting the corresponding ligands with [$PdCl_2(MeCN)_2$] in acetone for 15 h at rt or 2 h at 55 °C under air (Scheme 2). All

dx.doi.org/10.1021/ic5013999 | *Inorg. Chem.* 2014, 53, 9284−9295

Scheme 2. Synthesis of NBN-Pincer Ligands and Complexes[a]

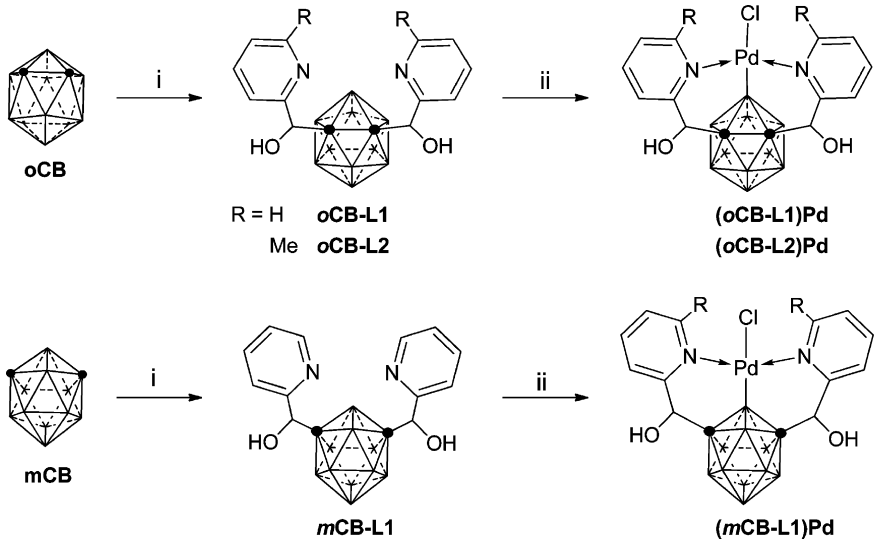

[a](i) *n*-BuLi, ether (0 °C), pyridinecarboxaldehyde (−94 °C for ***o*CB** or −63 °C for ***m*CB**), 4 h, H_2O, H^+; (ii) $PdCl_2(MeCN)_2$, acetone, rt/55 °C.

spectroscopic data are consistent with the proposed molecular structures (Scheme 1) and are in agreement with the solid-state molecular structures determined by single crystal X-ray diffraction methods (*vide infra*). The complexes precipitated from the reaction media as air stable pale yellow solids, soluble in very polar solvents such as DMF or DMSO (**(*m*CB-L1)Pd** being slightly more soluble than **(*o*CB-L1)Pd**). It was noted that pincer formation was somewhat easier for the ***o*CB-L1** ligand than that for the ***m*CB-L1** one. Introduction of a methyl group in the 6-position at the pyridine moieties (***o*CB-L2**) clearly decreased the reactivity of this ligand toward Pd(II), and only mixtures of a pincer complex with starting ligand were obtained. Thus, in the absence of steric hindrance, complexation to Pd(II) proceeds smoothly to enable B−H bond cleavage and biscyclopalladation to afford six-membered metallacycles, which are also typical for related aryl based Pd complexes with NCN ligands.[16] It is however worth noting that even though the B−H bond is inversely polarized compared to a typical C−H bond, pincer complex formation is observed after a few minutes in case of **(*o*CB-L1)Pd**. Similar facile B−H activation has been recently reported to occur in dicarboxylic acids of carboranes by iridium.[17]

X-ray Structural Analysis. The molecular structures for compounds **(*o*CB-L1)Pd**, **(*o*CB-L2)Pd** and **(*m*CB-L1)Pd** were unequivocally established by single crystal X-ray diffraction (Figure 2) and are in agreement with the NMR data (*vide infra*). Experimental crystal data and structure refinement parameters for the new pincer complex structures reported in this work are listed in Table 1. Whereas the *o*-carborane derivatives (**(*o*CB-L1)Pd** and **(*o*CB-L2)Pd**) both crystallize in the triclinic $P\bar{1}$ space group, the *m*-carborane compound (**(*m*CB-L1)Pd**) crystallizes in the monoclinic $P2_1/c$ space group. The molecular structures for all these pincer palladium complexes show typical icosahedrons with very similar bond distances and angles, and also similar to those in other *o*- or *m*-carboranyl alcohols.[14] The structure for the **(*o*CB-L1)Pd** complex shows that the *syn*-diasteroisomer (*meso*) has preferentially crystallized from the diastereisomeric mixture (top of Figure 2). On the other hand, the **(*o*CB-L2)Pd** and **(*m*CB-L1)Pd** structures crystallized as mixtures of *syn*- and *anti*-steroisomers with OH groups disordered over two positions (with site occupancy factors 0.863:0.137 for **(*o*CB-L2)Pd**) and 0.731:0.269 for **(*m*CB-L1)Pd**. The Pd(II) metal atoms display a strongly distorted square planar coordination: for complex **(*syn*-*o*CB-L1)Pd**, maximum distances from the least-squares plane are +0.163 Å for B(6), and −0.167/−0.165 for N(20)/N(28); for complex **(*m*CB-L1)Pd**, corresponding distances are +0.267 Å for B(2), and −0.256/−0.260 for N(20)/N(28); for complex **(*o*CB-L2)Pd**, the maximum distances are −0.119 Å for Pd(1), and +0.043 for B(3). In all complexes the two pyridine rings are in a *trans* fashion and a chloride atom is *trans* to the boron atom coordinated to Pd(II). Molecular structures for the complexes show unambiguously B−H activation of the carborane cages. Activation takes place in the B−H bonds close to the carborane carbon atoms, B(3/6)H in *o*-carborane or B(2/3)H in *m*-carborane (Figure 2). A comparison of selected bond distances and angles is shown in Table 2 for all structures in this work along with those for the only other two carborane pincer structures reported so far.[7]

The structures of compounds **(*syn*-*o*CB-L1)Pd**, **(*o*CB-L2)Pd**, and **(*m*CB-L1)Pd** display exceptionally long Pd−Cl distances in the solid state, suggesting a strong *trans* influence of the carborane moieties (Table 2). Such long Pd−Cl distances are sensibly longer than similar motifs in aryl-based pincers (2.39−2.45 Å)[18] and are comparable with that for related alkyl-based pincer Pd complexes (2.49−2.52 Å).[19] The Pd−B distances (1.97−2.02 Å) are also short and are consistent with a Pd−B σ bond as that found in the related *m*-carboranyls **1**−**2**.[8] To gain more insight into these new structural motifs, density functional theory (DFT) calculations were performed for all structures in this work and those previously reported by Mirkin.[8] Surprisingly, optimized structures of monomers of the compounds show systematically shorter Pd−Cl distances (and longer B−Pd distances) compared to the X-ray structures (Table 3). In the case of the related **(*syn*-*o*CB-L1)Pd** and **(*m*CB-L1)Pd** compounds, the computed Pd−Cl distances are shorter than the experimental values by 0.085 and 0.069 Å, respectively. Control calculations performed at different levels of theory (see Supporting Information) clearly indicate that the origin of this discrepancy is not due to the accuracy of the

dx.doi.org/10.1021/ic5013999 | *Inorg. Chem.* 2014, 53, 9284−9295

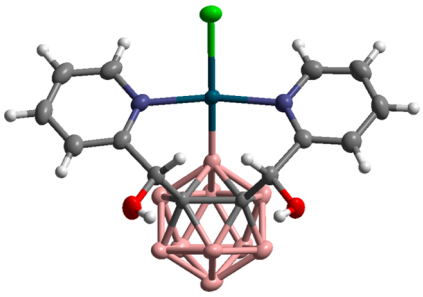

(*o*CB-L1)Pd

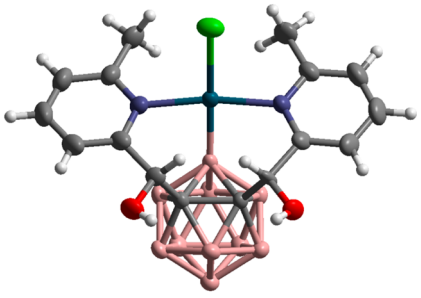

(*o*CB-L2)Pd

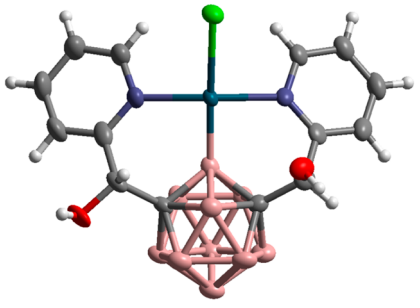

(*m*CB-L1)Pd

Figure 2. Molecular structures of (***o*CB-L1)Pd**, (***o*CB-L2)Pd**, and (***m*CB-L1)Pd**; thermal ellipsoids set at 90%, 70%, and 80% probability, respectively, and H atoms are represented as fixed-size spheres of 0.18 Å (B−H and pyridine hydrogen atoms are omitted for clarity). Color code: B pink; C gray; H white; O red; N blue; Cl green; Pd prussian blue. Only one stereoisomer is represented in those structures with disorder of OH groups.

chosen computational setup. Further analysis of the crystal structures reveals that the hydroxyl groups of a neighboring complex form H-bonds with the chloride ligand: (***syn-o*CB-L1)Pd** ($(O-H)_2\cdots Cl$, O···Cl 3.194(2)/3.098(2) Å; OHCl 156.5/157.4°), (***o*CB-L2)Pd** $(O-H)_2\cdots Cl$, O···Cl 3.177(2)/3.088(3) Å; OHCl 163.3/161.4°) and (***m*CB-L1)Pd** (O−H···Cl, O···Cl 2.997(3)/3.172(3) Å; OHCl 179.7/166.5°).[20] We thus set up calculations on the dimeric structure for (***syn-o*CB-L1)Pd** (no isomerism) and for (***m*CB-L1)Pd** (*syn* and *anti* isomers). H-bonded dimers of (***o*CB-L2)Pd** were not considered because of the high number of isomers. The computed Pd−Cl distances for the dimeric structures are now in good agreement with the experimental solid state data (Table 3). As a means of comparison, we also computed compounds **1** and **2** from Mirkin et al.[7] Inspection of the crystal structures shows intermolecular C−H···Cl interactions which are expected to be weaker than the O−H···Cl H-bonds observed in the crystal structures of (***syn-o*CB-L1)Pd**, (***o*CB-L2)Pd**, and (***m*CB-L1)Pd**. Accordingly, calculations on the monomeric and oligomeric states (a trimer for **1** and dimer for **2**; see Supporting Information for details) provide similar optimized geometric parameters, in fair agreement with the experimental data. It thus appears that two effects are operative in modulating the Pd−Cl distance in the crystal structures. One is the *trans* influence of the carborane moieties, the other being the intermolecular moderate H-bonding interactions among neighboring complexes. This finding is certainly relevant since the length of the metal−Cl bonds is often the only parameter considered for evaluating the *trans* influence in metal complexes. Calculations clearly show that in the absence of strong intermolecular interactions, like in the case of **1** and **2**, the Pd−Cl distances in the crystals can be a direct measure of the *trans* influence. The situation is however different when moderate intermolecular hydrogen bonding is taking place as it is the case of (***syn-o*CB-L1)Pd**, (***o*CB-L2)Pd**, and (***m*CB-L1)Pd**. The Cl atoms are acting as H-bonding acceptors with the consequent elongation of the Pd−Cl bond. Therefore, calculated distances for the isolated molecules in the gas phase (in the absence of intermolecular H-bonding) can be taken as a more appropriate indication of *trans* influence than the X-ray distances in our complexes. Thus, considering the Pd−Cl distances from the gas phase calculated monomers (Table 3), it can be inferred a stronger *trans* influence of the *m*-carborane than the *o*-carborane moieties in the pincer complexes, as expected. Such calculated Pd−Cl distances are therefore suggesting a *trans* influence for the carborane moieties in (***syn-o*CB-L1)Pd**, (***o*CB-L2)Pd**, and (***m*CB-L1)Pd** similar to that found in aryl-based pincers.[16]

We have applied an orbital localization procedure to further investigate the extent of intramolecular *trans* influence and intermolecular H-bond contribution.[21] Specifically, we have used the displacement of the localized orbital centroid (Wannier centers) to quantify each contribution. The approach has been successfully used in the literature to characterize environment effects[22] on bonding interactions and to develop ionicity scales.[23] Furthermore, Sit et al. proposed to use the localized orbital centroids to determine the oxidation state of transition metal ions.[24] Recently, we have reported that the approach is capable of providing valuable insight in the analysis of the electronic structure of organometallic compounds.[25] In summary, the localization procedure that we employ provides the centroid of charge (Wannier centers) and the spread of each orbital. This allows visualizing a picture of "where" electrons are and "who" they belong to. Selected localized orbitals for pincer complex (***syn-o*CB-L1)Pd** and the corresponding free ligand ***syn-o*CB-L1**, with their corresponding orbital centroids, are shown in Figure 3. Table 3 collects the charges and orbital centroids for all calculated compounds.

Inspection of the localized orbital for the Pd−B bond of (***syn-o*CB-L1)Pd** (middle of Figure 3) reveals a pear-shaped orbital centered on the boron atom of the carborane ligand, which would suggest a dative bond. However, the orbital centroid (green dot in Figure 3) for the Pd−B bond is located at about the center of the Pd−B bond, as expected for a covalent bond. On the contrary, the centroid of the Pd−Cl bond is clearly closer to the chloride, as expected for a strongly polarized bond on the basis of the respective (Pauling) electronegativities. Table 3 shows that the same is observed for all complexes. Quite interestingly, the elongation of the Pd−Cl bonds on intermolecular H-bond formation is followed by a concomitant

dx.doi.org/10.1021/ic5013999 | *Inorg. Chem.* 2014, 53, 9284−9295

Table 1. Crystal Data and Refinement Details for Structures of Compounds *syn-o*CB-Pd1, *o*CB-Pd2, and *m*CB-L1[a]

	(*syn-o*CB-L1)Pd	(*o*CB-L2)Pd	(*m*CB-L1)Pd
empirical formula	$C_{38}H_{70}B_{20}C_{l4}N_8O_6Pd_3$	$C_{16}H_{25}B_{10}ClN_2O_2Pd$	$C_{17}H_{28}B_{10}ClN_3O_3Pd$
formula weight	1412.22	527.33	572.37
crystal system	triclinic	triclinic	monoclinic
space group	$P\bar{1}$	$P\bar{1}$	$P2_1/c$
temperature/K	100.0	100.0	100.0
wavelength/Å	0.71073	0.71073	0.71073
a/Å	10.6774(5)	9.9166(4)	11.0330(5)
b/Å	10.9800(4)	10.7176(4)	20.3495(10)
c/Å	13.2409(6)	12.7142(5)	11.0094(5)
α/deg	99.934(2)	68.9240(10)	90
β/deg	101.468(2)	67.4490(10)	96.4690(18)
γ/deg	102.624(2)	67.4990(10)	90
volume/Å^3	1446.22(11)	1116.52(8)	2456.0(2)
Z	1	2	4
density (calculated)/ Mg/m^3	1.622	1.569	1.548
F(000)	708	528	1152
theta range for data collection/deg	2.41−26.37	2.32−26.37	2.672−26.371
absorption coefficient/mm^{-1}	1.159	0.969	0.891
goodness-of-fit on F^2	1.080	1.065	1.123
R_1 [$I > 2\sigma(I)$]	0.0226	0.0239	0.0334
wR_2 [$I > 2\sigma(I)$]	0.0572	0.0643	0.0765
R_1 (all data)	0.0247	0.0249	0.0429
wR_2 (all data)	0.0581	0.0649	0.0810

[a]CCDC 1008023 (*syn-o*CB-L1)Pd), 1008024 ((*o*CB-L2)Pd), and 1008025 ((*m*CB-L1)Pd) contain the supplementary crystallographic data for this paper. These data can be obtained free of charge from The Cambridge Crystallographic Data Centre via www.ccdc.cam.ac.uk/data_request/cif.

Table 2. Comparison of Selected Distances (Å) and Angles (deg) for (*syn-o*CB-L1)Pd, (*o*CB-L2)Pd, and (*m*CB-L1)Pd and 1−2

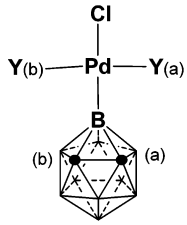

Y = N

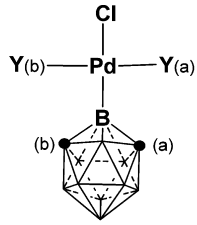

Y = N Y = S Y = Se

	Y = N		Y = N	Y = S	Y = Se
	(*syn-o*CB-L1)Pd	(*o*CB-L2)Pd	(*m*CB-L1)Pd	1	2
Pd−Cl	2.4915(5)	2.4879(6)	2.5063(8)	2.417(1)	2.4371(5)
Pd−B	2.021(2)	2.017(2)	1.974(4)	1.983(4)	1.982(3)
Pd−Y(a)	2.0557(17)	2.0490(18)	2.088(3)	2.3113(9)	2.4252(3)
Pd−Y(b)	2.0564(18)	2.0477(18)	2.087(3)	2.3204(9)	2.4340(3)
Cc(a)−B	1.718(3)	1.730(3)	1.704(5)	1.707(5)	1.714(3)
Cc(b)−B	1.723(3)	1.730(3)	1.706(5)	1.693(6)	1.720(4)
Cl−Pd−B	175.14(7)	171.85(7)	170.98(10)	173.1(1)	171.09(7)
Y−Pd−Y	166.76(7)	170.35(7)	161.55(10)	162.70(3)	162.11(1)

displacement of the Wannier centers of the Pd−Cl bonds. Thus, the intermolecular H-bonds are significantly affecting the orbitals of the Pd−Cl bonds, confirming their role on the exceptionally long distances found in the solid structures. Concerning the Pd−Cl bonds of the isolated molecules in the gas phase, we note that the longest Pd−centroid distance is displayed by (*m*CB-L1)Pd, consistent also with the idea that the ***m*CB-L1** ligand has the strongest *trans* influence. To further characterize the nature of the interactions, we have performed a natural bond orbital (NBO) analysis for our complexes (Table S3 in Supporting Information).[26] The results suggest in this case that the Pd−B bond is better described as covalent, whereas the Pd−Cl is clearly ionic.

It was suggested that the Pd in these carboryl pincer compounds might be formally Pd(0), based on calculated Mulliken and Löwdin charges for **2**.[8] The authors found a net negative charge localized on the Pd atom and a relative positive charge concentrated on the B atom bonded to it (B(2); see Figure 2 for nomenclature). However, they recognized that only the Löwdin charges showed some consistency and stressed the importance of being cautious in the choice of functional, effective core potentials and in the (quantitative) interpretation

dx.doi.org/10.1021/ic5013999 | Inorg. Chem. 2014, 53, 9284−9295

Table 3. Calculated Geometrical, Atomic Charges and Electronic Parameters for Selected Atoms in Compounds (*syn*-*o*CB-L1)Pd, (*o*CB-L2)Pd, (*m*CB-L1)Pd, and 1−2

	(*syn*-*o*CB-L1)Pd	(*syn*-*o*CB-L1)Pd (dimer)	(*o*CB-L2)Pd	(*m*CB-L1)Pd	(*m*CB-L1)Pd (dimer)	1	1 (trimer)	2	2 (dimer)
				Distances (Å)					
Pd−Cl	2.406	2.502	2.430	2.437	2.497 (*anti*) 2.505 (*syn*)	2.402	2.419	2.422	2.443
Pd−B	2.046	2.043	2.043	2.002	1.992 (*anti*) 1.987 (*syn*)	2.004	1.998	2.012	2.011
				Charges (Bader)					
Pd	0.280	0.248	0.241	0.247	0.237 (*anti*) 0.240 (*syn*)	0.060	−0.001	0.007	−0.002
Cl	−0.616	−0.624	−0.615	−0.638	−0.639 (*anti*) −0.642 (*syn*)	−0.607	−0.610	−0.608	−0.622
B	0.856	0.911	0.746	1.254	1.330 (*anti*) 1.345 (*syn*)	1.205	1.318	1.238	1.374
				Localized Orbital Centroids					
Pd−X−Cl	1.733/0.676	1.902/0.603	1.750/0.680	1.782/0.655	1.886/0.611 (*anti*) 1.897/0.608 (*syn*)	1.721/0.681	1.765/0.656	1.757/0.666	1.802/0.642
Pd−X−B	1.014/1.032	0.930/1.114	1.010/1.037	0.975/1.027	0.924/1.069 (*anti*) 0.919/1.069 (*syn*)	0.946/1.059	0.929/1.069	0.951/1.061	0.925/1.086
Pd oxidation state	II	II	II	II	II	II	II	II	II

of the results. For comparison, we have therefore calculated Mulliken, Löwdin and Bader and NPA charges for ours and Mirkin's pincer complexes (Table S2 in Supporting Information). In general, Mulliken and Löwdin charges suggest a negative Pd and a positive B atom bonded to it, in line with Mirkin's findings.[8] On the contrary, Bader and NPA charges suggest positive charges on both Pd and boron atom. It may be appreciated that Mulliken, Löwdin and Bader's charges describe B as more positive than Pd, whereas within the NPA description Pd is more positively charged. These results suggest that interpreting the oxidation state of the metal based on calculated charges is certainly delicate. Thus, we have employed the electron counting procedure proposed by Sit et al.,[24] which is based on the assignment of localized orbital centroids to individual atoms, for ours and Mirkin pincer complexes. This method suggests a Pd(II) state for all carboranyl pincer complexes as eight centroids (d^8 configuration) are clearly localized around the Pd atoms. Certainly, the different assignment of the Pd oxidation state depends on the nature of the Pd−B bond. Figure 3 shows the localized orbitals corresponding to the Pd−B bond in (***syn*-*o*CB-L1)Pd** and H−B bond in the free ligand *syn*-***o*CB-L1**. It may be appreciated the inversion of the polarity of the bond from the H−B (centroid close to H) to the Pd−B (centroid in the middle), consistent with the idea that the electrons involved in the Pd−B bond "belong" to boron. Thus, based on the above electron counting procedure and the shape of the Pd−B localized orbital, we assigned the corresponding orbital centroid to B, resulting in a Pd(II) oxidation state.

Characterization of Carborane-Based NBN Pincer Complexes. All spectroscopic and analytical data are consistent with the proposed molecular structures (Scheme 2) and are in agreement with the solid-state structures determined by single crystal X-ray diffraction methods (Figure 2). ^{11}B NMR spectroscopy shows a unique very broad resonance (ranging from δ +10 to −20) centered at $\delta \approx -6$ and −11 for the (***o*CB-Ln)Pd** (n = 1, 2) and (***m*CB-L1)Pd**, respectively. The broadness of the ^{11}B NMR signals, probably a consequence of the diastereomeric mixtures, prevent the direct observation of typical singlet resonance for the boron atom bonded to metals at $\delta \approx 0$.[8] Coordination of the Pd ion leads to a general downfield shift of signals of the free ligands in the ^{1}H NMR spectra, this being consistent with related Pd complexes. ^{11}B-decoupled ^{1}H NMR spectra shows also broad resonances for the hydrogen atoms at the boron atoms that are reasonable sharp, compared to the coupled spectra, so that integration is possible unless residual solvent signals overlap occurs. Thus, ^{1}H{^{11}B} NMR for the free ligand ***o*CB-L1** shows broad resonances for 10 boron atoms in the range δ 3 to 1.3.[14d] The pattern in the related complex (***o*CB-L1)Pd** changes to four resonances for nine boron atoms in a 1:3:3:2 ratio and in a larger range (δ 2.7 to 0.4). The introduction of Pd into ***o*CB-L1** modifies the symmetry of the carborane cluster, and this consequently modifies the observed pattern for the hydrogens at boron atoms. It is noteworthy the strongly deshielded resonance for two BH hydrogens at δ 0.4 (respect to the closest resonance at δ 1.9). The upfield signals are likely due to the shielding cone of the pyridine rings, and we tentatively assigned to hydrogens attached to B(4) and B(7). The related B(6/11) H hydrogens for (***o*CB-L2)Pd** also appears upfield (δ 0.24). The situation is more complex for the *m*-carboryl pincer (***m*CB-L1)Pd** since B−H activation for the mixture of *syn*- and *anti*-diastereoisomers afford four possible isomers (see Supporting

dx.doi.org/10.1021/ic5013999 | Inorg. Chem. 2014, 53, 9284−9295

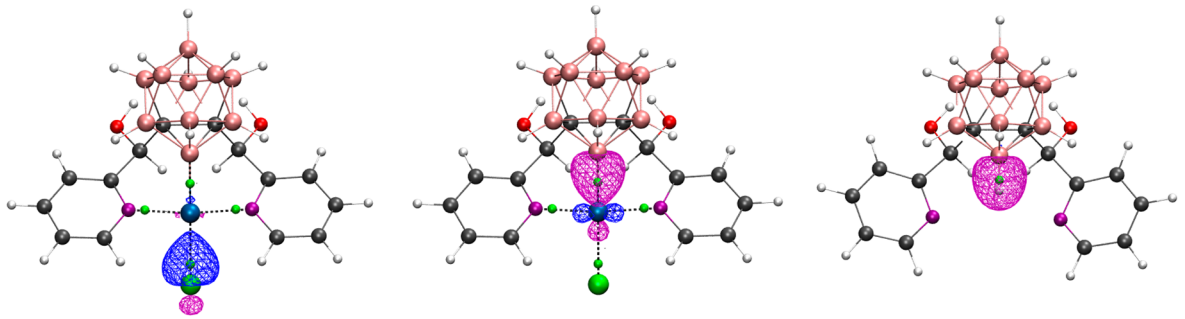

Figure 3. Localized orbitals corresponding to the Pd−Cl, Pd−B, and H−B bonds of (*syn*-*o*CB-L1)Pd (left and middle) and *syn*-*o*CB-L1 (right), respectively. The orbital centroids of the localized orbitals at the Pd center are shown as small green dots.

Information for details). As mentioned above, the *m*CB-L1 ligand is obtained as a mixture of *syn*- and *anti*-diasteromers and shows a unique set of signals in the ^{1}H NMR, probably due to free rotation of the pyridylmethylalcohol arms around the Cc-C bonds (Cc: carbon cluster). Rotation is not possible on complexation so that diastereomers formation is evident from the ^{1}H NMR spectrum for the Pd complex (*m*CB-L1)Pd. The ^{1}H NMR spectrum for a mixture of *anti*- and *syn*-diastereoisomers of (*m*CB-L1)Pd, as obtained in the synthesis, shows two sets of signals for the CHOH groups in a ∼1:1 ratio as doublets at δ 5.14 and 4.96. Although pyridine and OH signals for the mixture of four diastereoisomers results in a quite complicated spectrum, integration shows the expected ratio of signals.

Carborane-Based NBN Pincer Complexes As Catalysts. We have initiated a systematic study on the use of the newly synthesized carboranyl NBN pincer Pd complexes as homogeneous catalysts. The catalytic profile of both (*o*CB-L1)Pd and (*m*CB-L1)Pd was evaluated in one of the most important Pd-catalyzed C−C bond-forming processes, the Suzuki-Miyaura cross-coupling reaction.[27] Accordingly, the coupling of two common substrates, 4-methoxyphenylboronic acid and 4-bromoacetophenone, was chosen as model reaction using (*o*CB-L1)Pd as palladium source. As displayed in Table 4, from the full range of experimental conditions assayed with a catalyst loading of 0.1 mol %, we learned that the use of water as reaction media interestingly provided better results (entry 10 vs 1−8) than those from organic solvents and partially aqueous mixtures (THF, DMF, MeOH, THF/H_2O, MeOH/H_2O), far more suitable to solubilize carboranyl-based pincer (*o*CB-L1)Pd. Considering the excellent conversion rate obtained, which was not improved by the use of TBAB, a known stabilizing agent for palladium nanoparticles,[28] we decided to further decrease the catalyst amount down to 0.0001 mol %. A quantitative result was again obtained at such a low level (entry 16), and accordingly a range of substrates were submitted to the optimized reaction conditions (K_2CO_3, H_2O, 110 °C, 10 h) using (*o*CB-L1)Pd and (*m*CB-L1)Pd (Table 5). No coupling was observed in the absence of the pincer complex (entry 17, Table 4) and ICP-MS analysis of all the reagents employed (aryl halide, boronic acid, potassium carbonate) revealed that the palladium contents in the reaction mixture were around 10^{-5} mol %. Therefore, the possibility of a coupling catalyzed by residual palladium traces from the reagents was ruled out.

Although more assays should be carried out in order to determine the scope of the procedure, the comparative study of the catalytic activity of both pincer complexes displayed in Table 5 reveals that not only arylboronic acids can be effectively coupled with aryl bromides but also potassium phenyltrifluoroborate (Table 5, entries 3, 5, 7, and 10). In addition, benzyl bromide can be also used as a coupling partner (entries 11−14), and both electron-withdrawing and -donating groups can be incorporated in the substrates. No byproducts were observed, and apart from the coupling products, only unreacted halides were detected in the crude reaction mixtures. With a few exceptions (entries 4, 11, and 13), a better catalytic profile was observed from (*o*CB-L1)Pd-containing aqueous solutions, since (*m*CB-L1)Pd failed to provide the corresponding biaryl compound with acceptable yields in some cases (entries 6 and 8).

Table 4. Summary of Reactions Conditions for the Coupling between 4-Bromoacetophenone and 4-Methoxyphenylboronic Acid

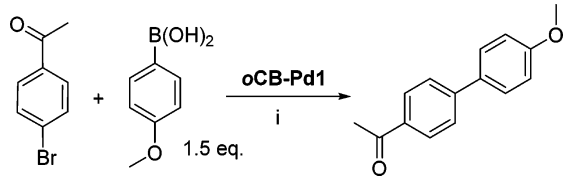

entry	reaction conditions (i)[a]	conv (%)[b]
1	KOH (2.5 equiv), THF, 40 °C, 10 h	-
2	K_2CO_3 (2.0 equiv), TBAB (1 equiv), THF, 40 °C, 12 h	10
3	K_3PO_4 (2 equiv), DMF, 80 °C, 10 h	5
4	K_2CO_3 (2.0 equiv), CH_3OH/H_2O (3:1), 70 °C, 12 h	-
5	K_2CO_3 (2.5 equiv), TBAB (1 equiv), CH_3OH, 70 °C, 10 h	68
6	K_2CO_3 (2.0 equiv), CH_3OH, 70 °C, 10 h	66
7	Cs_2CO_3 (2.5 equiv), H_2O, 100 °C, 12 h	7
8	K_2CO_3 (2.0 equiv), THF/H_2O (9:1), 80 °C, 10 h	88
9	Et_3N (2.0 equiv), H_2O, 80 °C, 12 h	99
10	K_2CO_3 (2.0 equiv), H_2O, 110 °C, 10 h	99
11[c]	K_2CO_3 (2.5 equiv), TBAB (1 equiv), CH_3OH, 70 °C, 10 h	62
12[c]	K_2CO_3 (2.5 equiv), TBAB (1 equiv), CH_3OH, 100 °C, 10 h	63
13[c]	K_2CO_3 (2.0 equiv), CH_3OH, 70 °C, 10 h	60
14[c]	K_2CO_3 (2.0 equiv), THF/H_2O (9:1), 80 °C, 10 h	84
15[c]	Et_3N (2.0 equiv), H_2O, 80 °C, 12 h	95
16[c]	K_2CO_3 (2.0 equiv), H_2O, 110 °C, 10 h	99
17[d]	K_2CO_3 (2.0 equiv), H_2O, 110 °C, 10 h	-

[a]4-Bromoacetophenone, 4-methoxyphenylboronic acid (1.5 equiv), (*o*CB-L1)Pd (10^{-1} mol %), base (2−3 equiv), solvent (1 mL per mmol of substrate), additive (when indicated). [b]Conversion rate measured by GC-MS. [c](*o*CB-L1)Pd (10^{-4} mol %). [d]Reaction performed in the absence of (*o*CB-L1)Pd.

dx.doi.org/10.1021/ic5013999 | Inorg. Chem. 2014, 53, 9284−9295

Table 5. Suzuki Coupling in the Presence of Carborane-Based NBN Pincer Complexes. Functional Group Tolerance

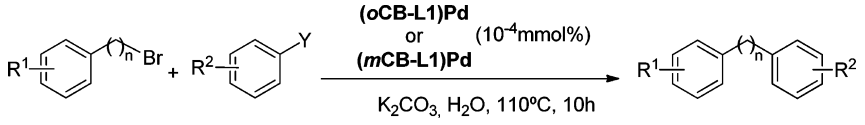

Entry	R^1	R^2	n	Y	(*o*CB-L1)Pd (%)[a]	(*m*CB-L1)Pd (%)[a]
1	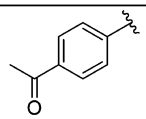	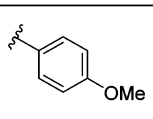	0	$B(OH)_2$	99	60
2	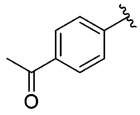		0	$B(OH)_2$	99	85
3[b]	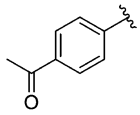		0	BF_3K	99	93
4	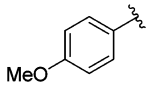		0	$B(OH)_2$	84	90
5[b]	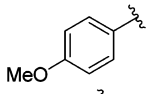		0	BF_3K	92	60
6			0	$B(OH)_2$	91	5
7[b]			0	BF_3K	97	69
8		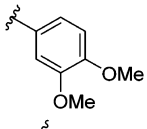	0	$B(OH)_2$	77	20
9	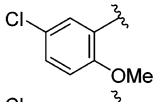		0	$B(OH)_2$	66	56
10[b]	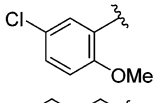		0	BF_3K	61	54
11	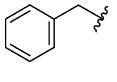	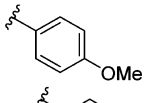	1	$B(OH)_2$	82	99
12	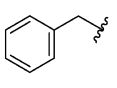	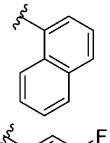	1	$B(OH)_2$	99	99
13	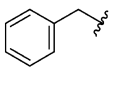	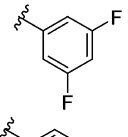	1	$B(OH)_2$	87	95
14	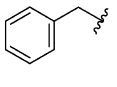	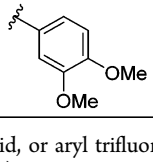	1	$B(OH)_2$	99	99

[a]Aryl or arylmethyl bromide, arylboronic acid, or aryl trifluoroborate (1.5 equiv), (*o*CB-L1)Pd or (*o*CB-L1)Pd (10^{-4} mol %), K_2CO_3 (2.0 equiv), H_2O (1 mL per mmol of ArBr or $ArCH_2Br$), 110 °C, 10 h. Isolated yields. [b]2.5 equiv of K_2CO_3 were used.

TON values ranged from 770000 to 990000 for (*o*CB-L1)Pd, thus showing a very high catalytic activity which rivals previous reports on Suzuki coupling performed by very low amounts of palladium catalysts, even with pincer complexes.[29]

dx.doi.org/10.1021/ic5013999 | Inorg. Chem. 2014, 53, 9284−9295

Moreover, the use of water as a convenient, sustainable solvent is an added bonus that cannot be ignored.

The low catalytic loading employed prevented an analysis of the palladium species generated after the coupling reaction, including that related to possible changes in the structure of the carborane moieties. However, no palladium black or mirror was observed, even when the catalyst amount was increased at the 10^{-1} mol % level (Table 4, entry 10), which is to some extent indicative of the integrity of the metal complex under the reaction conditions. Although no detailed mechanistic studies have been carried out for the present Suzuki coupling reactions, it occurs to us that the catalytic activity in water and the elongation of the Pd−Cl bonds due to intermolecular H-bond formation might be connected. It seems feasible that intermolecular H-bond between the water molecules and chloride atoms in both pincer complexes take place under the catalytic conditions. In such case, the *trans* influence of *o*- versus *m*-carborane becomes negligible, and therefore a similar catalytic activity is found in both cases. We are currently investigating other catalytic reactions that might exploit the different *trans* influence of these carboranyl pincer complexes.

CONCLUSIONS

We report the preparation of the first family of *o*-carborane-based NBN pincer palladium complexes (***o*CB-L1)Pd** and (***o*CB-L2)Pd**, along with the related *m*-carborane-based NBN pincer complex (***m*CB-L1)Pd** by the reaction of bis-[R-(hydroxy)methyl]-1,2-dicarba-*closo*-dodecaborane (R = 2-pyridyl ***o*CB-L1**, 6-methyl-2-pyridyl ***o*CB-L2**) or bis-[2-pyridyl(hydroxy)methyl]-1,2-dicarba-*meta*-dodecaborane (***m*CB-L1**) with $PdCl_2(MeCN)_2$ under mild conditions. The X-ray structures of (***o*CB-L1)Pd**, (***o*CB-L2)Pd**, and (***m*CB-L1)Pd** shows that the Pd(II) metal atoms display a strongly distorted square planar coordination, the two pyridine rings are in a *trans* fashion and a chloride atom is *trans* to a boron atom coordinated to Pd(II). Molecular structures for the complexes show unambiguously B−H activation of the carborane cages. Activation takes place in the B−H bonds close to the carborane carbon atoms, B(3/6)H in *o*-carborane or B(2/3)H in *m*-carborane. A combined study of experimental and calculated bond distances reveals that two effects are operative in modulating the Pd−Cl distance in the crystal structures. One is the *trans* influence of the carborane moieties, the other being the intermolecular moderate H-bonding interactions among neighboring complexes. This finding is certainly relevant since the length of the metal−Cl bonds are often the only parameter considered for evaluating the *trans* influence in metal complexes. Thus, considering the Pd−Cl distances from the gas phase calculated monomers, it can be inferred a stronger *trans* influence of the *meta*-carborane than the *ortho*-carborane moieties in the pincer complexes, as expected, and similar to that found in aryl-based pincers. Calculated atomic charges and localized orbitals have been used to analyze the nature of the Pd−B bond and the metal oxidation state in our *o*- and *m*-carboranyl pincer complexes but also in the previously reported *m*-carborane-based EBE (E = S, Se) pincer Pd complexes.[8] The results agree with the Pd−B bonds in all complexes exhibiting strong σ-electron donation and suggest that the Pd atom in all these carboryl pincer complexes bear a formal oxidation state of two, rather than zero, as previously suggested.[8] Catalytic applications of (***o*CB-L1)Pd** and (***m*CB-L1)Pd** have shown the complexes are good catalyst precursors in Suzuki coupling reactions in water and with remarkably low amounts of catalyst loadings and with good functional group tolerance for the substrates. Complex (***o*CB-L1)Pd** shows a better catalytic profile than (***m*CB-L1)Pd** and with excellent conversions and TON values ranging from 770000 to 990000, thus showing a very high catalytic activity which rivals previous reports on Suzuki coupling performed by very low amounts of palladium catalysts, even with pincer complexes.

EXPERIMENTAL SECTION

Materials and Methods. Reactions were carried out under a nitrogen atmosphere in round-bottomed flasks equipped with a magnetic stirring bar, capped with a septum unless noted otherwise. Diethyl ether was distilled from Na/benzophenone. All the other chemicals were commercially available and used as received. ***o*CB-L1** was prepared according to our previous report.[14d] IR ATR spectra were recorded on a Perkin−Elmer Spectrum One spectrometer. ^{1}H, ^{13}C, and ^{11}B spectra were recorded respectively at 300, 75, and 96 MHz with a Bruker Advance-300 spectrometer in deuterated chloroform, acetone or dimethyl sulfoxide, and referenced to the residual solvent peak for ^{1}H and ^{13}C NMR or to $BF_3.OEt_2$ as an external standard for ^{11}B NMR. Chemical shifts are reported in ppm and coupling constants in Hertzs. Multiplets nomenclature is as follows: s, singlet; d, doublet; t, triplet; br, broad; m, multiplet. Elemental analyses were obtained by a CarboErba EA1108 microanalyzer (Universidad Autónoma de Barcelona). The mass spectra were recorded in the positive or negative ion mode using a BrukerBiflex MALDI-TOF-MS [N2 laser; λexc 337 nm (0.5 ns pulses); voltage ion source 20.00 kV (Uis1) and 17.50 kV (Uis2)] with 3,5-dimethoxy-4-hydroxycinnamic acid as matrix. ICP-MS analyses were conducted using a ICP-MS Thermo Serie X. Column chromatography was conducted on silica gel (gel (35−70 mesh, 60 Å).

Computational Details. DFT calculations and orbital localization were performed with the CP2K code[30] and based on the PBE exchange-correlation functional.[31] The Quickstep[32] algorithm was used to solve the electronic structure problem using a double-ζ plus polarization (DZVP)[33] basis set to represent valence orbitals and plane waves for the electron density (300 Ry cutoff). Valence-core interactions were treated by means of GTH-type pseudopotentials.[34−36] Wave function optimization was achieved through an orbital transformation method.[37] Models were treated as isolated[38] and optimized (until gradients were $<5 \times 10^{-4}$ a.u.). Full details on the localization algorithm as implemented in CP2K may be found in ref 39. Atomic electron populations have been computed integrating the orbital density within the atomic basins determined according to Bader's Atom in Molecules theory.[40]

*Synthesis of 1,2-Bis{(6-methyl-pyridin-2′-yl)methanol}-1,2-dicarba-closo-dodecaborane (**oCB-L2**).* The general procedure described by us for ***o*CB-L1** was followed,[14d] using *o*-carborane (207 mg, 1.44 mmol), *n*-BuLi (1.84 mL, 1.56 M in hexane, 2.87 mmol), diethyl ether (20 mL) and 6-methyl-2-pyridinecarboxaldehyde (0.23 mL, 2.90 mmol), and an ethyl acetate/liquid N_2 cooling bath (−84 °C). Work up gave a light yellow solid that was dried under vacuum to afford a mixture of ***syn***- and ***anti*-*o*CB-L2** (317.2 mg, 0.82 mmol, 57.3%); mp 175−180 °C. NMR experiments confirmed the presence of the two different diastereoisomers in a 45:55 proportion.

*NMR for **anti-oCB-L2**.* ^{1}H NMR (DMSO-d_6): 7.76 (t, J = 7.5, 2H, C_5H_3N), 7.39 (d, J = 7.6, 2H, C_5H_3N), 7.24 (d, J = 7.3, 2H, C_5H_3N), 7.00 (d, J = 5.7, 2H, OH), 5.51 (d, J = 5.6, 2H, C*H*OH), 2.50 (CH_3 signals are overlapped with residual DMSO). ^{11}B NMR: −2.4 (s, 2B), −9.8 (b s, 8B).

*NMR for **syn-oCB-L2**.* ^{1}H NMR (DMSO-d_6): 7.76 (t, J = 8.0, 2H, C_5H_3N), 7.35 (d, J = 7.8, 2H, C_5H_3N), 7.24 (d, J = 7.8, 2H, C_5H_3N), 6.94 (d, J = 5.7, 2H, OH), 5.88 (d, J = 6.0, 2H, C*H*OH), 2.50 (CH_3 signals are overlapped with residual DMSO). ^{11}B NMR: −2.4 (s, 2B), −9.8 (b s, 8B).

*Synthesis of 1,7-Bis{(pyridin-2′-yl)methanol}-1,7-dicarba-closo-dodecaborane (**mCB-L1**).* The general procedure described by us for ***o*CB-L1** was followed,[14d] using *m*-carborane (200 mg, 1.38 mmol), *n*-BuLi (1.86 mL, 1.48 M in hexane, 2.76 mmol), THF (10 mL) and 2-

dx.doi.org/10.1021/ic5013999 | Inorg. Chem. 2014, 53, 9284−9295

pyridinecarboxaldehyde (0.27 mL, 2.83 mmol), and an chloroform/liquid N_2 cooling bath ((−63 °C). Work up gave a light yellow solid which was dried under a vacuum to afford a mixture of *syn*- and *anti*-**mCB-L1** (369.6 mg, 1.03 mmol, 79.3%), mp 145−150 °C. IR (ATR; selected bands): ν 3379 (OH), 2613, 2595, 2554 (BH). MALDI TOF: 359.10 $[M + H]^+$. NMR of the diastereoisomer mixture in various solvents:

(Ac-d_6). ^{1}H NMR: 8.51 (d, J = 3.0, 1H, C_5H_4N), 7.81 (td, J = 9.0 and 3.0, 1H, C_5H_4N), 7.42 (d, J = 6.0, 1H, C_5H_4N), 7.36(td, J = 6.0 and 3.0, 1H, C_5H_4N),5.40 (d, J = 6.0, 1H, OH), 4.96 (d, J = 6.0, 1H, CHOH). ^{1}H {^{11}B} NMR (Ac-D_6): Only signals due to B−H protons are given: 2.73 (br s, 2H), 2.19 (br s, 2H), 2.15 (br s, 3H), 1.88 (br s, 3H); ^{11}B NMR: −5.34 (br s, 2B), −10.61 (br s, 6B), −12.98 (br s, 2B). ^{13}C NMR: 160.17 (s, NC_5H_4), 148.99 (s, NC_5H_4), 137.42 (s, NC_5H_4), 124.43 (s, NC_5H_4), 122.83 (s, NC_5H_4), 82.45 (s, cluster Carbons), 75.31 (s, CHOH).

(DMSO-d_6). ^{1}H NMR: 8.45 (d, J = 5.0 Hz, 2H, C_5H_4N), 7.80 (t, J = 7.4, 1.5, 2H, C_5H_4N), 7.35 (d, J = 8.0, 2H, C_5H_4N), 7.30 (dd, J = 7.5, 4.7, 2H, C_5H_4N), 6.50 (d, J = 5.7, 2H, OH), 4.80 (d, J = 5.3, 2H, *C*HOH). ^{1}H{^{11}B} NMR: Only signals due to B−H protons are given: 2.60 (br s, 2H), 2.06 (br s, 6H), 1.79 (br s, 2H). −5.13 (br s, 2B), −10.66 (br s, 6B).

*Synthesis of [(**o**CB-L1)PdCl] ((**o**CB-L1)Pd)*. ***o*CB-L1** (100 mg, 0.28 mmol) and $PdCl_2(MeCN)_2$ (61 mg, 0.28 mmol) were dissolved in acetone (10 mL) in a capped vial. The reaction mixture was stirred under air at room temperature for 15 h. Then a yellowish precipitate was collected by centrifugation (6000 rpm, 10 min), washed with acetone (3 × 3 mL) to remove excess of starting materials, and dried under a vacuum to provide pure **(*o*CB-L1)Pd** (100 mg, 0.2 mmol, 71%) as a pale yellow solid; dec pt 283 °C. Elemental analysis calculated for $C_{14}B_{10}H_{21}N_2O_2ClPd{\cdot}H_2O$: C 32.50%, H 4.48%, N 5.42%; found C 32.52%, H 4.20%, N 5.42%. MALDI-TOF, m/z: M: 462.45 $[M - Cl\text{-}H]^+$. IR (ATR; selected bands): ν 3344, 3316 (OH), 2617, 2594, 2567, 2553 (BH). ^{1}H NMR (DMSO-d_6): δ = 8.92 (d, J = 4.9, 2H, NC_5H_4), 8.14 (t, J = 7.6, 2H, NC_5H_4), 7.90 (d, J = 7.3, 2H, NC_5H_4), 7.55 (t, J = 6.7, 2H, NC_5H_4), 7.45 (BR s, 2H, CHO*H*), 6.09 (BR s, 2H, *C*HOH); ^{1}H{^{11}B} NMR (DMSO-d_6): Only signals due to B−H protons are given: 2.75 (br s, 1H), 2.17 (br s, 3H), 1.86 (br s, 3H), 0.39 (br s, 2H); ^{11}B NMR (DMSO-d_6): +10 to −20 (br m). ^{13}C NMR (DMSO-d_6): 161.01 (s, NC_5H_4), 153.39 (s, NC_5H_4), 139.65 (s, NC_5H_4), 124.49 (s, NC_5H_4), 123.52 (s, NC_5H_4), 89.93 (s, CHOH), 72.37 (s, $CHB_{10}H_9$).

*Synthesis of [(**o**CB-L2)PdCl] ((**o**CB-L2)Pd)*. The reaction procedure of **(*o*CB-L1)Pd** was followed, using ***o*CB-L2** (10 mg, 0.028 mmol), $[PdCl_2(MeCN)_2]$ (6.1 mg, 0.028 mmol), and acetone (3 mL), under air at 55 °C for 50 h. Work up gave **(*o*CB-L2)Pd** as an impure white solid. Recrystallization from DMF gave single crystals suitable for X-ray diffraction measurements. MALDI-TOF, m/z: M: 491.52 $[M]^+$. ^{1}H NMR (DMSO-d_6): 8.02 (t, J = 7.8, 2H, C_5H_3N), 7.71 (d, J = 7.2, 2H, C_5H_3N), 7.51 (d, J = 7.3, 2H, C_5H_3N), 7.45 (br s, 2H, OH), 6.18 (br s, 2H, CHOH), 3.15 (s, 6H, CH_3). ^{1}H {^{11}B} NMR (DMSO-d_6): Only signals due to B−H protons are given: 2.77−2.12 (br m, overlapped with residual solvent), 1.84 (br s, 3H), 0.24 (br s, 2H); ^{11}B NMR (DMSO-d_6): −2.41 (br s, 10B) 5 to −20 (br m).^{13}C NMR (DMSO-d_6): 160.28 (s, C_5H_3N), 153.27 (s, C_5H_3N), 139.41 (s, C_5H_3N), 124.97 (s, C_5H_3N), 120.55 (s, C_5H_3N), 90.38 (s, cluster carbon), 71.89 (s, CHOH), 27.02 (s, CH_3).

*Synthesis of [(**m**CB-L1)PdCl] ((**m**CB-L1)Pd)*. The reaction procedure of **(*o*CB-L1)Pd** was followed, using ***m*CB-L1** (10 mg, 0.028 mmol), $[PdCl_2(MeCN)_2]$ (6.1 mg, 0.028 mmol) and acetone (3 mL), under air at 55 °C for 2 h. Work up gave pure **(*m*CB-L1)Pd** (10.6 mg, 0.021 mmol, 76.1%) as a light yellow solid; dec pt 282 °C. Elemental analysis calculated for $C_{14}B_{10}H_{21}N_2O_2ClPd{\cdot}DMF$: C 35.67%, H 4.93%, N 7.34%; found C 35.76%, H 5.08%, N 7.10%. MALDI-TOF, m/z: M: 462.49 $[M - Cl\text{-}H]^+$. IR (ATR; selected bands): ν 3412, 3178 (OH), 2603 (BH). ^{1}H NMR (DMSO-d_6): 10.02, 9.91, 9.82, and 9.68 (d, J = 5.7, 2H, C_5H_3N for four diasteromers), 8.10−7.49 (m, 6H, C_5H_3N), 7.08, 7.07, 6.91, and 6.83 (d, J = 5.9, 2H, OH for for four diasteromers), 5.14 (d, J = 5.9, 1H, *C*HOH for ***anti***- or ***syn*-mCB-Pd1** isomer), 4.96 (d, J = 5.3, 1H, *C*HOH for ***syn***- or ***anti*-mCB-Pd1** isomer). ^{11}B NMR (DMSO-d_6): −11.4 (br m). ^{13}C NMR (DMSO-d_6): 162.24, 161.16, 160.96, 157.81, 155.76, 154.69, 139.74, 139.53, 139.40, 127.32, 124.22, 123.58, 122.88, 122.61 (s, NC_5H_4), 76.11, 75.74, 75.35, 74.47, 73.92, 73.75 (s, CHOH and $CHB_{10}H_9$).

Suzuki Coupling with Arylboronic Acids in the Presence of (*o*CB-L1)Pd. General Procedure. A screw-capped tube equipped with a magnetic stirrer bar was charged with the aryl- or benzyl bromide (1 mmol), arylboronic acid (1.5 mmol), potassium carbonate (276 mg, 2.0 mmol), and **(*o*CB-L1)Pd** (0.00049 mg, 10^{-6} mmol) and distilled water (1 mL) at room temperature. This mixture was heated to 110 °C for 10 h under stirring, allowed to cool, and extracted with diethyl ether (4 × 5 mL). The combined organic extracts were dried over anhydrous sodium sulfate and evaporated *in vacuo* to give a residue that was purified by flash column chromatography using hexane:ethyl acetate as eluent. By this procedure the following biaryls and diarylmethanes were prepared:

4-Acetyl-4′-methoxybiphenyl[41] *(99%)*. ^{1}H NMR ($CDCl_3$) δ: 2.63 (s, 3H), 3.86 (s, 3H), 7.01 (d, J = 8.8 Hz, 2H), 7.57 (d, J = 8.8 Hz, 2H), 7.65 (d, J = 8.4 Hz, 2H), 7.99 (d, J = 8.4 Hz, 2H). ^{13}C NMR ($CDCl_3$) δ 26.6, 55.3, 114.4, 126.6, 128.3, 128.9, 132.2, 135.2, 145.3, 159.9, 197.7

4-Acetylbiphenyl[42] *(99%)*. ^{1}H NMR ($CDCl_3$) δ: 8.03 (d, J = 8.0 Hz, 2H), 7.68 (d, J = 8.0 Hz, 2H), 7.62 (d,J = 7.6 Hz, 2H), 7.47 (t, J = 7.6 Hz, 2H), 7.41 (d, J = 7.6 Hz, 1H), 2.65 (s, 3H). ^{13}C NMR ($CDCl_3$): δ 197.7, 145.7, 139.8, 135.8, 128.9, 128.8, 128.2, 127.2, 127.1, 26.7.

4-Methoxybiphenyl[21] *(84%)*. ^{1}H NMR ($CDCl_3$) δ: 7.56−7.51 (m, 4H), 7.41 (t, J = 7.6 Hz, 2H), 7.30 (t, J = 7.6 Hz, 1H), 6.98 (d, J = 7.2 Hz, 2H), 3.85 (s, 3H). ^{13}C NMR ($CDCl_3$) δ: 159.1, 140.8, 133.7, 128.7, 128.1, 126.7, 126.6, 114.2, 55.3.

2-Chloridebiphenyl[21] *(91%)*. ^{1}H NMR ($CDCl_3$) δ: 7.48−7.38 (m, 6H), 7.36−7.26 (m, 3H). ^{13}C NMR ($CDCl_3$) δ: 140.5, 139.4, 132.5, 131.4, 129.9, 129.4, 128.5, 128.0, 127.6, 126.8.

2-Chloro-3′,4′-dimethoxy-1,1′-biphenyl[43] ***(77%)***. ^{1}H NMR ($CDCl_3$) δ: 3.87, 3.89 (2s, 6H), 6.94 (d, J = 8.4 Hz, 1H), 7.08 (d, J = 2.0 Hz, 1H), 7.12 (dd, J = 8.2, 2.2 Hz, 1H), 7.39−7.52 (m, 4H). ^{13}C NMR ($CDCl_3$) δ: 148.6, 148.4, 140.3, 132.6, 132.1, 131.4, 130.0, 128.3, 126.8, 121.8, 112.9, 110.8, 56.0, 55.9.

5-Chloro-2-methoxy-1,1′-biphenyl[44] *(66%)*. ^{1}H NMR ($CDCl_3$) δ: 7.52 (m, 2H), 7.37 (m, 5H), 6.92 (d, J = 8.4 Hz, 1H), 3.81 (s, 3H). ^{13}C NMR ($CDCl_3$) δ: 155.9, 155.1, 137.1, 132.4, 130.4, 129.3, 128.1, 128.05, 127.4, 125.7, 112.5.

1-Benzyl-4-methoxybenzene[45] *(82%)*. ^{1}H NMR ($CDCl_3$) δ: 3.81 (s, 3H), 3.96 (s, 2H), 6.86 (d, J = 8.5 Hz, 2H), 7.18 (d, J = 8.5 Hz, 2H), 7.24−7.29 (m, 3H), 7.32 (t, J = 7.3 Hz, 2H). ^{13}C NMR ($CDCl_3$) δ: 41.2, 55.4, 114.0, 126.1, 128.6, 129.0, 130.0, 133.4, 141.7, 158.1.

1-Benzylnaphthalene[46] *(99%)*. ^{1}H NMR ($CDCl_3$) δ: 4.53 (s, 2H), 7.24−7.31 (m, 3H), 7.32−7.40 (m, 3H), 7.47−7.56 (m, 3H), 7.85 (d, J = 8.4 Hz, 1H), 7.91−9.97 (m, 1H), 8.05−8.12 (m, 1H).^{13}C NMR ($CDCl_3$) δ: 39.2, 124.4, 125.7, 126.1, 126.2, 127.5, 127.5, 128.6, 128.8, 128.9, 132.3, 134.1, 136.8, 140.8.

1-Benzyl-3,5-difluorobenzene[47] *(87%)*. ^{1}H NMR ($CDCl_3$) δ: 7.33 (tt, J = 8.2, 1.6 Hz, 2H), 7.25 (tt, J = 6.2, 1.4 Hz, 1H), 7.20−7.17 (m, 2H), 6.74−6.68 (m, 2H), 6.65 (tt, J = 9.0, 2.3 Hz, 1H), 3.96 (s, 2H). ^{13}C NMR ($CDCl_3$) δ: 163.0 (dd, J_{C-F} = 248.0, 12.9 Hz), 145.0 (t, J_{C-F} = 8.9 Hz), 139.4, 128.9, 128.7, 126.6, 111.6 (dd, J_{C-F} = 18.4, 6.5 Hz), 101.6 (t, J_{C-F} = 25.4 Hz), 41.6 (t, J_{C-F} = 1.9 Hz). ^{19}F NMR (376 MHz, $CDCl_3$) δ: −110.3 (m, 2F)

4-Benzyl-1,2-dimethoxybenzene[48] *(99%)*. ^{1}H NMR ($CDCl_3$) δ: 3.84−3.87 (2 s, 6H), 3.96 (s, 3H), 6.74−6.83 (m, 3H), 7.20−7.34 (m, 5H). ^{13}C NMR ($CDCl_3$) δ: 41.4, 55.7, 55.8, 111.1, 111.2, 112.2, 120.7, 120.8,125.9, 128.3, 128.6, 133.5, 141.2, 147.3, 148.8.

Suzuki Coupling with Potassium Phenyltrifluoroborate in the Presence of (*o*CB-L1)Pd. General Procedure. A screw-capped tube equipped with a magnetic stirrer bar was charged with the aryl bromide (1 mmol), potassium phenyltrifluoroborate (276 mg, 1.5 mmol), potassium carbonate (276 mg, 2.0 mmol), and **(*o*CB-L1)Pd** (0.00049 mg, 10^{-6} mmol) and distilled water (1 mL) at room temperature. This mixture was heated to 110 °C for 10 h under

dx.doi.org/10.1021/ic5013999 | *Inorg. Chem.* 2014, 53, 9284−9295

stirring, allowed to cool, and extracted with diethyl ether (4 × 5 mL). The combined organic extracts were dried over anhydrous sodium sulfate and evaporated *in vacuo* to give a residue which was purified by flash column chromatography using hexane:ethyl acetate as eluent. By this procedure the following biaryls were prepared:

4-Acetylbiphenyl (99%)
4-Methoxybiphenyl (92%)
2-Chloridebiphenyl (97%)
5-Chloro-2-methoxy-1,1′-biphenyl (61%)

Suzuki Coupling with Arylboronic Acids in the Presence of *m*CB-Pd1. General Procedure. A screw-capped tube equipped with a magnetic stirrer bar was charged with the aryl- or benzyl bromide (1 mmol), arylboronic acid (1.5 mmol), potassium carbonate (276 mg, 2.0 mmol), and **(*m*CB-L1)Pd** (0.0005 mg, 10^{-6} mmol) and distilled water (1 mL) at room temperature. This mixture was heated to 110 °C for 10 h under stirring, allowed to cool, and extracted with diethyl ether (4 × 5 mL). The combined organic extracts were dried over anhydrous sodium sulfate and evaporated *in vacuo* to give a residue which was purified by flash column chromatography using hexane/ethyl acetate as eluent. By this procedure the following biaryls and diarylmethanes were prepared:

4-Acetyl-4′-methoxybiphenyl (60%)
4-Acetylbiphenyl (85%)
4-Methoxybiphenyl (90%)
2-Chloridebiphenyl (5%)
2-Chloro-3′,4′-dimethoxy-1,1′-biphenyl (20%)
5-Chloro-2-methoxy-1,1′-biphenyl (56%)
1-Benzyl-4-methoxybenzene (99%)
1-Benzylnaphthalene (99%)
1-Benzyl-3,5-difluorobenzene (95%)
4-Benzyl-1,2-dimethoxybenzene (99%)

Suzuki Coupling with Potassium Phenyltrifluoroborate in the Presence of (*m*CB-L1)Pd. General Procedure. A screw-capped tube equipped with a magnetic stirrer bar was charged with the aryl bromide (1 mmol), potassium phenyltrifluoroborate (276 mg, 1.5 mmol), potassium carbonate (276 mg, 2.0 mmol), and **(*m*CB-L1)Pd** (0.0005 mg, 10^{-6} mmol) and distilled water (1 mL) at room temperature. This mixture was heated to 110 °C for 10 h under stirring, allowed to cool, and extracted with diethyl ether (4 × 5 mL). The combined organic extracts were dried over anhydrous sodium sulfate and evaporated *in vacuo* to give a residue which was purified by flash column chromatography using hexane:ethyl acetate as eluent. By this procedure the following biaryls were prepared:

4-Acetylbiphenyl (93%)
4-Methoxybiphenyl (60%)
2-Chloridebiphenyl (69%)
5-Chloro-2-methoxy-1,1′-biphenyl (54%)

Single Crystal Studies. Crystals of **(*o*CB-L1)Pd**, **(*o*CB-L2)Pd**, and **(*m*CB-L1)Pd** were kept under inert conditions and immersed in perfluoropolyether as protecting oil for manipulation. A suitable size crystal was mounted on a MiTeGen Micromount, and this sample was used for data collection. Data were collected with a Bruker D8 Venture diffractometer (Mo$K\alpha$, 100 K). Data were processed with APEX2[49] suite and corrected for absorption using SADABS.[50] The structure was solved by direct methods,[51] which revealed the position of all non-hydrogen atoms. These atoms were refined on F^2 by a full-matrix least-squares procedure using anisotropic displacement parameters.[49] All hydrogen atoms were located in difference Fourier maps, except those corresponding to C−H groups which were placed geometrically, and included as fixed contributions riding on attached atoms with isotropic thermal displacement parameters 1.2 (C−H, B−H) or 1.5 (O−H, methyl) times those of the respective bonded atom. The structures of ***o*CB-Pd2** and ***m*CB-L1** exhibit disorder of the OH groups, which was successfully refined using a two-site model with 0.863:0.137 and 0.731:0.269 occupancies for ***o*CB-Pd2** and ***m*CB-L1**, respectively. Thermal parameter constraints were applied. The crystal of ***m*CB-L1** is a nonmerohedral twin with a minor component of 12.37%. The twin law describes a rotation of 180° around the [1 $\bar{1}$ 0] direction, given by the matrix (0.109 −0.887 0, −1.114 −0.109 0, 0 −0.014 −1). Absorption correction was applied using TWINABS.[52]

■ ASSOCIATED CONTENT

Ⓢ Supporting Information

Spectroscopic and crystallographic data. DFT functional calibration, atomic charges, and optimized geometries. This material is available free of charge via the Internet at http://pubs.acs.org.

■ AUTHOR INFORMATION

Corresponding Author

*E-mail: jginerplanas@icmab.es.

Notes

The authors declare no competing financial interest.

■ ACKNOWLEDGMENTS

We thank CICYT (Projects CTQ2010-16237 and CTQ2011-23336) and Generalitat de Catalunya (2009/SGR/00279) for financial support. M.Y.T. is enrolled in the UAB Ph.D. program. The project "Factoría de Cristalización, CONSOLIDER INGENIO-2010" provided X-ray structural facilities for this work. The evaluation of the catalytic activity was supported by the Basque Government (IT-774-13 and S-PC13UN018), the Spanish Ministry of Science and Innovation (CTQ2010-20703), and the University of the Basque Country (UFI QOSYC 11/12). N.C. thanks the Basque Government for a predoctoral scholarship. The authors also thank Petronor, S.A. for a generous donation of hexane.

■ REFERENCES

(1) See for example: (a) Selander, N.; Szabó, K. J. *Chem. Rev.* **2011**, *111*, 2048. (b) Moreno, I.; SanMartin, R.; Inés, B.; Churruca, F.; Domínguez, E. *Inorg. Chim. Acta* **2010**, *363*, 1903. (c) *The Chemistry of Pincer Compounds*; Morales-Morales, D., Jensen, C. M., Eds.; Elsevier: Amsterdam, 2007. (d) van der Boom, M.; Milstein, D. *Chem. Rev.* **2003**, *103*, 1759. (e) Albrecht, M.; van Koten, G. *Angew. Chem., Int. Ed.* **2001**, *40*, 3750.

(2) (a) Moulton, C. J.; Shaw, B. L. *J. Chem. Soc., Dalton Trans.* **1976**, 1020. (b) Poverenov, E.; Efremenko, I.; Frenkel, A. I.; Ben-David, Y.; Shimon, L. J. W.; Leitus, G.; Konstantinovski, L.; Martin, J. M. L.; Milstein, D. *Nature* **2008**, *455*, 1093. (c) Schuster, E. M.; Botoshansky, M.; Gandelman, M. *Angew. Chem., Int. Ed.* **2008**, *47*, 4555. (d) Goldman, A. S.; Roy, A. H.; Huang, Z.; Ahuja, R.; Schinski, W.; Brookhart, M. *Science* **2006**, *312*, 257.

(3) (a) Liang, L. C. *Coord. Chem. Rev.* **2006**, *250*, 1152. (b) Fan, L.; Foxman, B. M.; Ozerov, O. V. *Organometallics* **2004**, *23*, 326. (c) Fryzuk, M. D. *Can. J. Chem.* **1992**, *70*, 2839.

(4) (a) Dixon, L. S. H.; Hill, A. F.; Sinha, A.; Ward, J. S. *Organometallics* **2014**, *33*, 653. (b) Korshin, E. E.; Leitus, G.; Shimon, L. J. W.; Konstantinovski, L.; Milstein, D. *Inorg. Chem.* **2008**, *47*, 7177. (c) MacInnis, M. C.; MacLean, D. F.; Lundgren, R. J.; MacDonald, R.; Turculet, L. *Organometallics* **2007**, *26*, 6522. (d) Sangtrirutnugul, P.; Tilley, T. D. *Organometallics* **2007**, *26*, 5557.

(5) Mankad, N. P.; Rivard, E.; Harkins, S. B.; Peters, J. C. *J. Am. Chem. Soc.* **2005**, *127*, 16032.

(6) Teixidor, F.; Romerosa, A.; Viñas, C.; Rius, J.; Miravittles, C.; Casabó, J. *J. Chem. Soc. Chem. Commun.* **1991**, 192.

(7) Segawa, Y.; Yamashita, M.; Nozaki, K. *J. Am. Chem. Soc.* **2009**, *131*, 9201.

(8) Spokoyny, A. M.; Reuter, M. G.; Sterm, C. L.; Ratner, M. A.; Seideman, T.; Mirkin, C. A. *J. Am. Chem. Soc.* **2009**, *131*, 9482.

(9) (a) Spokoyny, A. M. *Pure Appl. Chem.* **2013**, *85*, 903. (b) Kameo, H.; Nakazawa, H. *Chem.—Asian J.* **2013**, *8*, 1720. (c) van der Vlugt, J. I. *Angew. Chem., Int. Ed.* **2010**, *49*, 252.

(10) El-Zaria, M. E.; Arii, H.; Nakamura, H. *Inorg. Chem.* **2011**, *50*, 4149.
(11) (a) Grimes, R. N. *Carboranes*, 2nd ed; Elsevier: Amsterdam, 2011). (b) Scholz, M.; Hey-Hawkins, E. *Chem. Rev.* **2011**, *111*, 7035. (e) Chizhevsky, I. T. *Coord. Chem. Rev.* **2007**, *251*, 1590. (f) Teixidor, F.; Viñas, C. In *Science of Synthesis*; Thieme: Stuttgart, 2005; Vol. *6*, p 1235. (g) Xie, Z. *Acc. Chem. Res.* **2003**, *36*, 1. (h) Valliant, J. F.; Guenther, K. J.; King, A. S.; Morel, P.; Schaffer, P.; Sogbein, O. O.; Stephensen, K. *Coord. Chem. Rev.* **2002**, *232*, 173. (i) Hawthorne, M. F.; Zheng, Z.-P. *Acc. Chem. Res.* **1997**, *30*, 267. (j) Plešek, J. *Chem. Rev.* **1992**, *92*, 269. (k) Bregadze, V. I. *Chem. Rev.* **1992**, *92*, 209.
(12) Hermansson, K.; Wójcik, M.; Sjöberg, S. *Inorg. Chem.* **1999**, *38*, 6039.
(13) (a) Spokoyny, A. M.; Machan, C. W.; Clingerman, D. J.; Rosen, M. S.; Wiester, M. J.; Kennedy, R. D.; Stern, C. L.; Sarjeant, A. A.; Mirkin, C. A. *Nat. Chem.* **2011**, *3*, 590. (b) Teixidor, T.; Barberà, G.; Vaca, A.; Kivekäs, R.; Sillanpää, R.; Oliva, J.; Viñas, C. *J. Am. Chem. Soc.* **2005**, *127*, 10158.
(14) (a) Terrasson, V.; Planas, J. G.; Prim, D.; Viñas, C.; Teixidor, F.; Light, M. E.; Hursthouse, M. B. *J. Org. Chem.* **2008**, *73*, 9140. (b) Terrasson, V.; García, Y.; Farràs, P.; Teixidor, F.; Viñas, C.; Planas, J. G.; Prim, D.; Light, M. E.; Hursthouse, M. B. *CrystEngComm* **2010**, *12*, 4109. (c) Di Salvo, F.; Planas, J. G.; Camargo, B.; Garcia, Y.; Teixidor, F.; Viñas, C.; Light, M. E.; Hursthouse, M. B. *CrystEngComm* **2011**, *13*, 5788. (d) Di Salvo, F.; Paterakis, C.; Tsang, M. T.; Viñas, C.; Teixidor, F.; Planas, J. G.; Light, M. E.; Hursthouse, M. B.; Choquesillo-Lazarte, D. *Cryst. Growth Des.* **2013**, *13*, 1473−1484.
(15) (a) Di Salvo, F.; Tsang, M. Y.; Teixidor, F.; Viñas, C.; Planas, J. G.; Crassous, J.; Vanthuyne, N.; Aliaga-Alcalde, N.; Ruiz, E.; Clevers, S.; Dupray, V.; Choquesillo-Lazarte, D.; Light, M. E.; Hursthouse, M. B. *Chem.—Eur. J.* **2014**, *20*, 1081−1090. (b) Di Salvo, F.; Teixidor, F.; Viñas, C.; Planas, J. G. *Z. Anorg. Allg. Chem.* **2013**, *639*, 1194. (c) Di Salvo, F.; Teixidor, F.; Viñas, C.; Planas, J. G.; Light, M. E.; Hursthouse, M. B.; Aliaga-Alcalde, N. *Cryst. Growth Des.* **2012**, *12*, 5720.
(16) Albrecht, M.; van Koten, G. *Angew. Chem., Int. Ed.* **2001**, *40*, 3750.
(17) Yaho, Z.-J.; Yu, W.-B.; Lin, Y.-J.; Huang, S.-L.; Li, Z. H.; Jin, G.-X. *J. Am. Chem. Soc.* **2014**, *136*, 2825.
(18) Selected examples of $NC_{aryl}N$-pincer palladium: (pyrido[2′,3′:5,6]naphtho[2,3-h]quinolin-14-yl)PdCl, Pd−Cl 2.4304(17) Å, Young, K. J. H.; Bu, X.; Kaska, W. C. *J. Organomet. Chem.* **2011**, *696*, 3992−3997. (2-(pyridin-2-yl)-6-((pyridin-2-yl)sulfanyl)phenyl)PdCl, Pd−Cl 2.4191(6) Å, Hirotsu, M.; Tsukahara, Y.; Kinoshita, I. *Bull. Chem. Soc. Jpn.* **2010**, *83*, 1058.); ((5*S*,7*S*)-2,6-bis(6,6-dimethyl-5,6,7,8-tetrahydro-5,7-methanoquinolin-2-yl)phenyl)PdCl, Pd−Cl 2.451(1) Å, Soro, B.; Stoccoro, S.; Minghetti, G.; Zucca, A.; Cinellu, M. A.; Manassero, M.; Gladiali, S. *Inorg. Chim. Acta* **2006**, *359*, 1879−1888. (2,6-bis(2-pyridyl)phenyl) PdCl, Pd−Cl 2.427(1) Å, Soro, B.; Stoccoro, S.; Minghetti, G.; Zucca, A.; Cinellu, M. A.; Gladiali, S.; Manassero, M.; Sansoni, M. *Organometallics* **2005**, *24*, 53−61. (4-bromo-2,6-bis(7-azaindolyl)-phenyl)PdCl, Pd−Cl 2.3867(16) Å, Song, D.; Wu, Q.; Hook, A.; Kozin, I.; Wang, S. *Organometallics* **2001**, *20*, 4683−4689.
(19) Selected examples of $NC_{alkyl}N$-pincer palladium: $(3,5\text{-}^{t}Bu_2pz)_2PdCl(Me)$, Pd−Cl 2.5165(9) Å, Li, K.; Darkwa, J.; Guzei, I. A.; Mapolie, S. F. *J. Organomet. Chem.* **2002**, *660*, 108−115. (N-N′)(h^2-olefin)PdCl(Me), Pd−Cl 2.492(1) Å, Albano, V. G.; Casterllari, C. *Organometallics* **1990**, *9*, 1269−1276.
(20) Intermolecular O−H···Cl hydrogen bonding for (***o*CB-L2**)**Pd** and (***m*CB-L1**)**Pd** have to be considered carefully due to the disorders in OH positition and as a consequence of the disatereoisomeric mixtures. See SI for details.
(21) Marzari, N.; Mostofi, A. A.; Yates, J. R.; Souza, I.; Vanderbilt, D. *Rev. Mod. Phys.* **2012**, *84*, 1419.
(22) Alber, F.; Folkers, G.; Carloni, P. *J. Phys. Chem. B* **1999**, *103*, 6121.
(23) Abu-Farsakh, H.; Qteish, A. *Phys. Rev. B* **2007**, *75*, 085201.
(24) Sit, P. H. L.; Zipoli, F.; Chen, J.; Car, R.; Cohen, M. H.; Selloni, A. *Chem.—Eur. J.* **2011**, *17*, 12136.
(25) Vidossich, P.; Lledos, A. *Dalton Trans.* **2014**, *43*, 11145−11151.
(26) Glendening, E. D.; Landis, C. R.; Weinhold, F. *WIREs Comput. Mol. Sci.* **2012**, *2*, 1.
(27) For an account on the relevance and widespread use of Suzuki coupling in academic, industrial research and bulky production, see: Martin, R.; Buchwald, S. L. *Acc. Chem. Res.* **2008**, *41*, 1461−1473.
(28) See for example: *Palladium-Catalyzed Coupling Reactions: Practical Aspects and Future Developments*; Molnar, A., Ed.; Wiley: Weinheim, 2013.
(29) (a) Beletskaya, I. P.; Cheprakov, A. V. *J. Organomet. Chem.* **2004**, *689*, 4055−4082. (b) Bolliger, J. L.; Blacque, O.; Frech, C. M. *Angew. Chem., Int. Ed.* **2007**, *46*, 6514−6517. (c) Inés, B.; SanMartin, R.; Moure, M. J.; Dominguez, E. *Adv. Synth. Catal.* **2009**, *351*, 2124−2132. (d) Rao, G. K.; Kumar, A.; Ahmedz, J.; Singh, A. K. *Chem. Commun.* **2010**, *46*, 5954−5956.
(30) VandeVondele, J.; Krack, M.; Mohamed, F.; Parrinello, M.; Chassaing, T.; Hutter, J. *Comput. Phys. Commun.* **2005**, *167*, 103.
(31) Perdew, J. P.; Burke, K.; Ernzerhof, M. *Phys. Rev. Lett.* **1996**, *77*, 3865.
(32) Lippert, G.; Hutter, J.; Parrinello, M. *Mol. Phys.* **1997**, *92*, 477.
(33) VandeVondele, J.; Hutter, J. Gaussian basis sets for accurate calculations on molecular systems in gas and condensed phases. *J. Chem. Phys.* **2007**, *127*, (11).
(34) Goedecker, S.; Teter, M.; Hutter, J. *Phys. Rev. B* **1996**, *54*, 1703.
(35) Hartwigsen, C.; Goedecker, S.; Hutter, J. *Phys. Rev. B* **1998**, *58*, 3641.
(36) Krack, M. *Theor. Chem. Acc.* **2005**, *114*, 145.
(37) VandeVondele, J.; Hutter, J. *J. Chem. Phys.* **2003**, *118*, 4365.
(38) Genovese, L.; Deutsch, T.; Neelov, A.; Goedecker, S.; Beylkin, G. *J. Chem. Phys.* **2006**, *125*, 074105.
(39) Berghold, G.; Mundy, C. J.; Romero, A. H.; Hutter, J.; Parrinello, M. *Phys. Rev. B* **2000**, *61*, 10040.
(40) Bader, R. F. W. *Acc. Chem. Res.* **1985**, *18*, 9.
(41) Liu, Q.-X.; Zhang, W.; Zhao, X.-J.; Zhao, Z.-X.; Shi, M.-C.; Wang, X.-G. *Eur. J. Org. Chem.* **2013**, 1253−1261.
(42) Zhou, W.-J.; Wang, K.-H.; Wang, J.-X.; Huang, D.-F. *Eur. J. Org. Chem.* **2010**, 416−419.
(43) McLean, M. R.; Bauer, U.; Amaro, A. R.; Robertson, L. W. *Chem. Res. Toxicol.* **1996**, *9*, 158−164.
(44) Bolligera, J. L.; Frecha, C. M. *Adv. Synth. Catal.* **2010**, *352*, 1075−1080.
(45) Molander, G. A.; Elia, M. D. *J. Org. Chem.* **2006**, *71*, 9198−9202.
(46) McLaughlin, M. *Org. Lett.* **2005**, *7*, 4875−4878.
(47) Burns, M. J.; Fairlamb, I. J. S.; Kapdi, A. R.; Sehnal, P.; Taylor, R. J. K. *Org. Lett.* **2007**, *9*, 5397−5400.
(48) Tsuchimoto, T.; Tobita, K.; Hiyama, T.; Fukazawa, S. *J. Org. Chem.* **1997**, *62*, 6997−7005.
(49) *Bruker, APEX2 Software*, V2012.2; Bruker AXS Inc.: Madison, WI, 2012.
(50) Sheldrick, G. M. *SADABS, Program for Empirical Absorption Correction of Area Detector Data*; University of Göttingen: Göttingen, Germany, 2012.
(51) Sheldrick, G. M. *Acta Crystallogr.* **2008**, *A64*, 112.
(52) Sheldrick, G. M. *TWINABS*; University of Göttingen, Germany, 2012.